



PCCP

**A Unified Reaction Network on the Formation of Five-Membered Ringed Polycyclic Aromatic Hydrocarbons (PAHs) and their Role in Ring Expansion Processes through Radical – Radical Reactions**

Journal:	<i>Physical Chemistry Chemical Physics</i>
Manuscript ID	CP-ART-11-2022-005305.R1
Article Type:	Paper
Date Submitted by the Author:	10-Jan-2023
Complete List of Authors:	Li, Wang; University of Science and Technology of China Zhao, Long; USTC, National Synchrotron Radiation Laboratory Kaiser, Ralf; University of Hawaii,

SCHOLARONE™  
Manuscripts

# **A Unified Reaction Network on the Formation of Five-Membered Ringed Polycyclic Aromatic Hydrocarbons (PAHs) and their Role in Ring Expansion Processes through Radical – Radical Reactions**

Wang Li,<sup>1</sup> Long Zhao,<sup>1,2\*</sup> Ralf I. Kaiser<sup>3\*</sup>

<sup>1</sup>*National Synchrotron Radiation Laboratory, University of Science and Technology of China, Hefei, Anhui 230029, China*

<sup>2</sup>*School of Nuclear Science and Technology, University of Science and Technology of China, Hefei, Anhui 230027, China*

<sup>3</sup>*Department of Chemistry, University of Hawaii at Manoa, Honolulu, HI 96822, USA*

## **Abstract**

Exploiting a chemical microreactor in combination with an isomer-selectively product identification through fragment-free photoionization utilizing tunable vacuum ultraviolet (VUV) light in tandem with the detection of the ionized molecules by a high resolution reflection time-of-flight mass spectrometer (Re-TOF-MS), the present investigation reveals molecular mass growth processes to four distinct polycyclic aromatic hydrocarbons carrying two six- and one five-membered ring ( $C_{13}H_{10}$ ): 3H-cyclopenta[a]naphthalene, 1H-cyclopenta[b]naphthalene, 1H-cyclopenta[a]naphthalene, and fluorene in the gas phase. Temperatures of 973 and 1,023 K simulating conditions in combustion settings along with circumstellar envelopes of carbon-rich stars and planetary nebulae. These reactions highlight the importance of methyl-substituted aromatic reactants (biphenyl, naphthalene) which can be converted to the methylene ( $-CH_2^*$ ) motive by hydrogen abstraction or photolysis. Upon reaction with acetylene, methylene-substituted aromatics carrying a hydrogen atom at the ortho position of the ring can be then converted to cyclopentadiene-annulated aromatics thus providing a versatile pathway to five-membered ring aromatics at elevated temperatures.

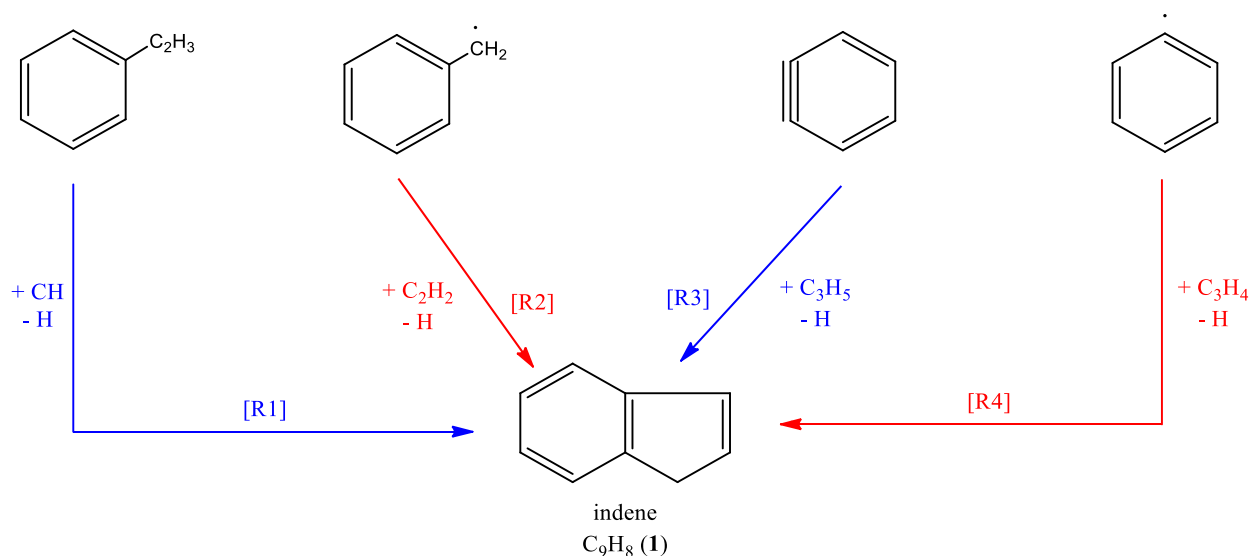
## 1. Introduction

The incorporation of a five-membered ring moiety in polycyclic aromatic hydrocarbons (PAHs) – a class of organic molecules composed of fused benzene rings with naphthalene ( $C_{10}H_8$ ) as the simplest representative - is fundamental to curve aromatic structures out of the molecular plane.<sup>1</sup> Aromatic molecules such as cyclopentanaphthalenes isomers ( $C_{13}H_{10}$ ) and fluorene ( $C_{13}H_{10}$ ) carry this five-membered carbon ring backbone and represent basic molecular building blocks of non-planar PAHs like corannulene ( $C_{20}H_{10}$ ) along with nanobowls ( $C_{40}H_{10}$ ,  $C_{50}H_{10}$ ) and fullerenes ( $C_{60}$ ,  $C_{70}$ ).<sup>2-16</sup> Therefore, an untangling of the elementary gas-phase reaction mechanisms toward five-membered ring PAHs is vital in our understanding of the very early chemistry in combustion systems<sup>17-22</sup> and in the evolution of carbon-rich circumstellar envelopes of aging Asymptotic Giant branch (AGB) stars such as IRC+10216<sup>23, 24</sup> together with planetary nebulae like TC 1 as their descendants.<sup>5, 25</sup> Exploiting crossed molecular beam experiments and chemical microreactor studies augmented by electronic structure calculations, the last decade revealed exciting progress in unraveling gas phase pathways to indene ( $C_9H_8$ , **1**) – the simplest aromatic molecule carrying one six-membered plus one five-membered ring (Scheme 1). The reactions involved [C1+C8], [C2+C7], and [C3+C6] systems spanning *styrene* ( $C_6H_5C_2H_3$ ) – *methylidyne* ( $CH$ ) [R1],<sup>5</sup> *benzyl* ( $C_6H_5CH_2$ ) – *acetylene* ( $C_2H_2$ ) [R2],<sup>1</sup> *o-benzyne* ( $C_6H_4$ ) – *allyl* ( $C_3H_5$ ) [R3],<sup>26</sup> as well as *phenyl* ( $C_6H_5$ ) – *methylacetylene/allene* ( $C_3H_4$ ) [R4],<sup>27-29</sup> respectively; those reactions denoted in italics have no entrance barrier and are exoergic and hence can efficiently operate even in cold molecular clouds (10 K) and in hydrocarbon rich atmospheres of planets and their moons such as Titan and Triton (40–140 K).<sup>30-32</sup>

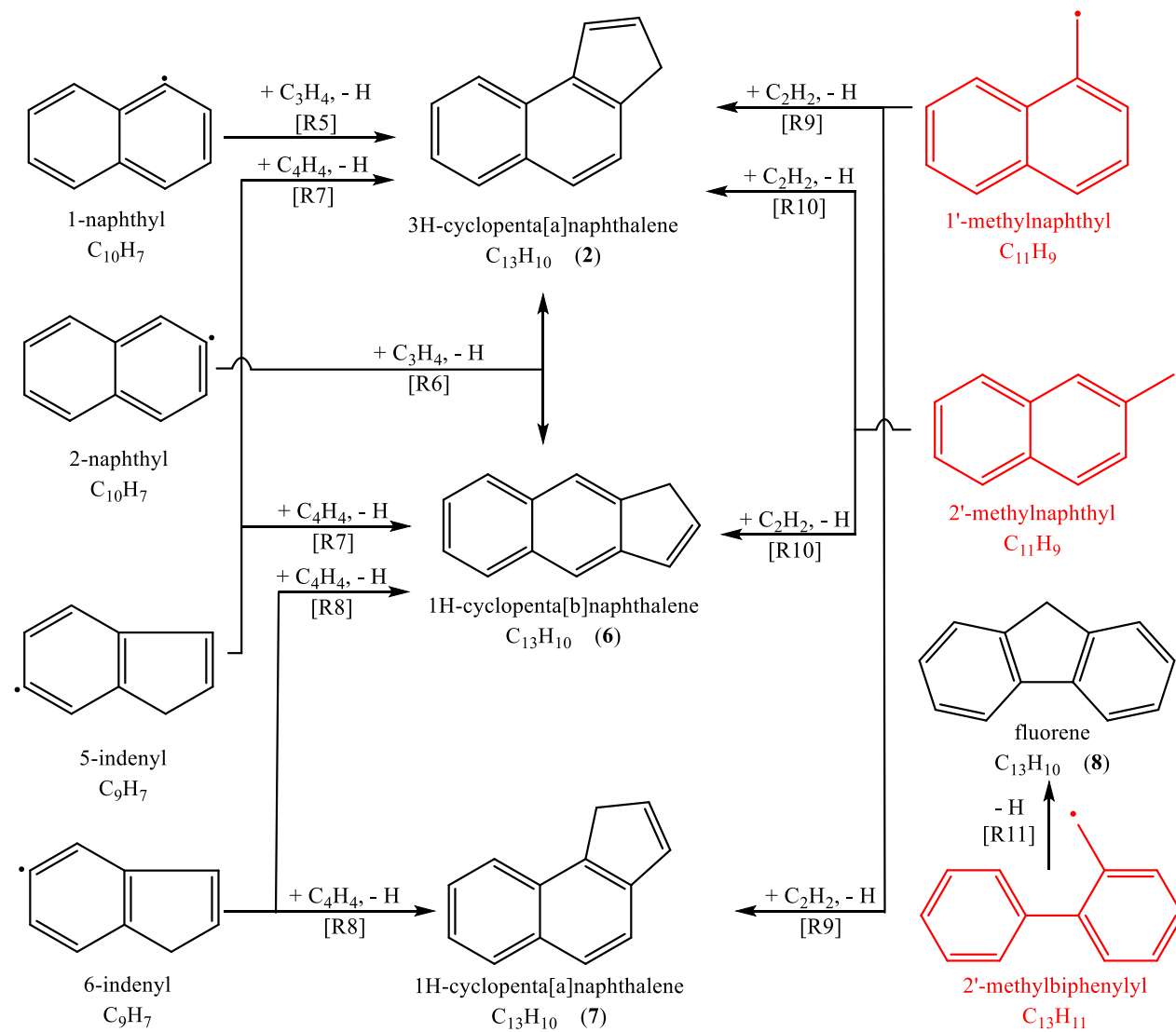
Whereas an understanding of the elementary reactions leading to indene ( $C_9H_8$ ) is beginning to emerge, the reaction mechanisms to cyclopentanaphthalenes (benzindenes,  $C_{13}H_{10}$ ) and fluorene ( $C_{13}H_{10}$ ), which can be formally derived by annulation of indene through a six-membered ring at the benzene or cyclopentadiene moieties, respectively, is less constrained (Scheme 2). Chemical microreactor studies revealed the formation of distinct cyclopentanaphthalenes (benzindenes,

$C_{13}H_{10}$  isomers through radical – hydrocarbon reactions covering [C3+C10] and [C4+C9] systems. For the [C3+C10] reactions [R5] and [R6], the radical center was located at the benzene moiety of the 1-/2-naphthyl ( $C_{10}H_7^\bullet$ ) with the hydrocarbon reactants allene/methylallene ( $C_3H_4$ ). The [C4+C9] systems [R7/R8] introduced the radical center via the 5-/6-indenyl ( $C_9H_7^\bullet$ ) radicals, which reacted with vinylacetylene ( $C_4H_4$ ). In detail, reactions of the naphthyl radicals [R5/R6] were found to produce 3H-cyclopenta[a]naphthalene (**2**) and 1H-cyclopenta[b]naphthalene (**6**) via five-membered ring annulation<sup>23, 33</sup> in analogy to the reaction of the phenyl radical ( $C_6H_5^\bullet$ ) with methylacetylene/allene ( $C_3H_4$ ) [R4].<sup>27, 28</sup> In case of the reaction with 1-naphthyl [R5], the aromatics acenaphthene ( $C_{12}H_{10}$ , **3**), methylacenaphthene ( $C_{13}H_{12}$ , **4**), and 1H-phenalene ( $C_{13}H_{10}$ , **5**) were also formed in the gas phase.<sup>33</sup> Compared to the [C3+C10] systems [R5/R6], which involved entrance barriers from 7.0 to 14.0 kJ·mol<sup>-1</sup>, the [C4+C9] systems [R7/R8] passed *submerged* barriers to addition of the radical center to the vinyl moiety of the vinylacetylene reactant following the Hydrogen Abstraction – Vinylacetylene Addition (HAVA) reaction mechanism.<sup>25, 30, 34-38</sup> These pathways eventually produced 3H-cyclopenta[a]naphthalene (**2**), 1H-cyclopenta[b]naphthalene (**6**), and 1H-cyclopenta[a]naphthalene (**7**) in barrierless and exoergic reactions.<sup>39</sup> However, elementary steps involving [C2+C11] systems are still elusive (Scheme 2). These pathways could form cyclopentanaphthalenes (benzindenes,  $C_{13}H_{10}$ ) via reactions of 1'-naphthylmethyl and 2'-naphthylmethyl ( $C_{11}H_9^\bullet$ ) [R9/R10] radicals with acetylene ( $C_2H_2$ ) leading to ring annulation in analogy to the benzyl-acetylene system forming indene (Scheme 1) [R2].<sup>1</sup> Finally, no reaction pathway to fluorene ( $C_{13}H_{10}$ , **8**) has been explored via molecular beams experiments [R11]. Recent identifications of benzindenes ( $C_{13}H_{10}$ ) in flames of ethylene ( $C_2H_4$ ),<sup>40, 41</sup> toluene ( $C_6H_5CH_3$ ),<sup>42-44</sup> and of benzene ( $C_6H_6$ )<sup>6</sup> highlight the combustion relevance of these species. Proposed mechanisms involve postulated multi step reactions of benzene ( $C_6H_6$ ) or phenyl ( $C_6H_5^\bullet$ ) with the benzyl radical ( $C_7H_7^\bullet$ ) accompanied by cyclization and formation of a five-membered ring. Alternatively, hydrogen abstraction from the methyl group of 1-methylnaphthalene ( $C_{11}H_{10}$ ) followed by acetylene reaction, isomerization, and hydrogen loss has been suggested to yield 3H-cyclopenta[a]naphthalene (**2**).<sup>42-44</sup>

The present investigation reveals the molecular mass growth processes to 3H-cyclopenta[a]naphthalene (**2**), 1H-cyclopenta[b]naphthalene (**6**), and fluorene (**8**) ( $C_{13}H_{10}$ ) via reactions [R9] to [R11] in the gas phase at elevated temperatures of 973 and 1,023 K simulating temperatures under combustion conditions along with circumstellar envelopes of carbon-rich stars and planetary nebulae. These studies exploit a chemical microreactor with products probed isomer-selectively through fragment-free photoionization utilizing tunable vacuum ultraviolet (VUV) light in tandem with the detection of the ionized molecules by a high resolution reflection time-of-flight mass spectrometer (Re-TOF-MS). These reactions highlight the critical role of methyl-substituted aromatic reactants (biphenyl, naphthalene): in combustion flames, open shell reactants such as atomic hydrogen can easily abstract a hydrogen atom from the methyl ( $-CH_3$ ) moiety generating molecular hydrogen along with the  $-CH_2^\bullet$  motive; in circumstellar environments and planetary nebulae, a photon may cleave the carbon-hydrogen bond forming aromatic and resonantly stabilized free radicals such as 1'-naphthylmethyl ( $C_{11}H_9^\bullet$ ) [R9], 2'-naphthylmethyl ( $C_{11}H_9^\bullet$ ) [R10], and 2'-methylbiphenyl ( $C_{13}H_{11}^\bullet$ ) [R11], which can then undergo ring annulation [R9/R10] and ring closure [R11], respectively.



Scheme 1: Reaction pathways exposed through molecular beam studies leading to indene (**1**). Barrierless routes are color coded in blue, whereas red colors indicate reactions with entrance barriers.



Scheme 2: Reaction pathways to distinct  $C_{13}H_{10}$  extracted from molecular beams experiments augmented by electronic structure calculations. Reactions [R9] to [R11] are subject of the present study with radical reactants highlighted in red.

## 2. Experimental

The experiments were performed at the BL03U beamline of the National Synchrotron Radiation Laboratory (NSRL) in Hefei, China, exploiting a chemical micro reactor (Fig. S1).<sup>45</sup> The chemical micro reactor consists of a silicon carbide (SiC) tube (40.0 mm long, 1.0 mm inner diameter, 2.0 mm outer diameter) connected to a stainless-steel Swagelok fitting through a graphite ferrule. A stainless-steel nozzle with an aperture of 0.1 mm is interfaced to the silicon carbide reactor. This nozzle system can be heated with the help of a heating jacket and a ceramic sleeve. The silicon carbide tube is resistively heated in the center of the reactor over a length of 20.0 mm with the temperature monitored through a type-S thermocouple. The distance between the end of the silicon carbide tube and the skimmer was optimized to 10.0 mm. After exiting the reactor, the continuous molecular beam passes a skimmer with the 2.0 mm diameter and then crosses the quasi-continuous tunable vacuum ultraviolet (VUV) light from the synchrotron. The products are photoionized and detected with a high resolution reflection time-of-flight mass spectrometer (ReTOF-MS) operated at a repetition rate of 33 kHz.<sup>45, 46</sup>

In experiment 1 [R9], a continuous beam of 1'-methyl-naphthyl ( $C_{11}H_9^{\bullet}$ ) radicals was prepared *in-situ* through the pyrolysis of 1'-chloromethylnaphthalene ( $C_{11}H_9Cl$ , Aladdin, > 95%). In detail, the solid precursor of 1'-chloromethylnaphthalene was placed in a stainless-steel filter (Swagelok, SS-6F-MM-05) equipped with a glass fiber heating belt. The filter was heated to 313 K as determined by a type-K thermocouple to promote the sublimation of solid 1'-chloromethylnaphthalene. The helium carrier gas (He) was controlled by an MKS mass flow controller at a rate of 20.0 ml/min (standard calibration) and was introduced into the filter; 1'-chloromethylnaphthalene was then seeded in the helium carrier gas and mixed with acetylene ( $C_2H_2$ , 10.0 ml/min) before eventually entering the SiC reactor at an inlet pressure of 350 Torr monitored by a PMS pressure sensor (PMS 111, BD Sensor Co., Ltd). The SiC reactor was resistively heated to  $1,023 \pm 10$  K measured by the type-S thermocouple. (Supplementary Material, Fig. S2a) Second, for experiment 2 [R10], the procedure is identical to experiment 1, but 2'-chloromethylnaphthalene ( $C_{11}H_9Cl$ , Aladdin, > 97%) was exploited as a precursor to 2'-methyl-naphthyl ( $C_{11}H_9^{\bullet}$ ) radicals with a flow rate of the helium carrier gas of 10.0 ml/min. The

total pressure at the inlet of the reactor was determined to be 250 Torr, while the temperature of the SiC reactor was maintained at  $973 \pm 10$  K. (Supplementary Material, Fig. S2a) Finally, for experiment 3 [R11], a quartz fiber dipped with the liquid precursor of 2-methylbiphenyl ( $C_{13}H_{12}$ , Aladdin, > 97%) was prepared in the filter (Swagelok, SS-6F-MM-05) and heated to 308 K by a heating tape. The homemade bubbler equipped with a thermostatic bath (Hangzhou Qiwei Instrument Co., Ltd) set at 288 K was adopted to contain oxalyl chloride ( $C_2Cl_2O_2$ , Aladdin, > 95%). The helium as carrier gas entered the filter and bubbler, respectively, with optimized flow rates of 10.0 and 20.0 ml/min. 2-Methylbiphenyl and oxalyl chloride were seeded in the helium carrier gas, respectively, and have a sufficient mix before entering the SiC reactor. The pressure of the gas mixture was maintained at 250 Torr; the SiC reactor was heated to  $1023 \pm 10$  K. The 2'-methylbiphenylyl radical ( $C_{13}H_{11}^{\bullet}$ ) was generated *in-situ* through hydrogen atom abstraction from the methyl group of 2-methylbiphenyl ( $C_{13}H_{12}$ ) by atomic chlorine generated in the pyrolysis of oxalyl chloride. (Supplementary Material, Fig. S2b) In order to demonstrate the performance of the newly developed *in-situ* radical source, a test experiment was conducted by introducing a mixture oxalyl chloride ( $C_2Cl_2O_2$ )/toluene ( $C_7H_8$ )/acetylene ( $C_2H_2$ ) into the SiC reactor. Hydrogen abstraction by atomic chlorine from the methyl group of toluene ( $C_7H_8$ ) leads to the benzyl radical ( $C_6H_5CH_2^{\bullet}$ ), which then reacted with acetylene ( $C_2H_2$ ) to indene ( $C_9H_8$ ) thus verifying the performance of our new radical source. (Supplementary Material, Section 2, Figs. S3-S4)

### 3. Results and Discussion

#### 3.1. Mass Spectra

Representative mass spectra of the experiments are presented in Fig. 1 for reactions [R9] (Figs.1a/b), [R10] (Figs. 1c/d), and [R11] (Figs. 1e/f). Blank experiments were also performed under identical conditions, but by substituting acetylene ( $C_2H_2$ ) (Figs. 1a/c) and oxalyl chloride ( $C_2Cl_2O_2$ ) with non-reactive helium (He) carrier gas (Fig. 1e). A comparison of the ion counts for the reactive systems [R9] (Fig. 1b) and [R10] (Fig.1d) with the corresponding blank experiments (Figs. 1a/c) provides compelling evidence on the formation of species with the molecular formula



$C_{13}H_9^\bullet$  ( $m/z = 165$ ) and  $^{13}CC_{12}H_9^\bullet/C_{13}H_{10}$  ( $m/z = 166$ ) in the 1'- and 2'-chloromethylnaphthalene ( $C_{11}H_9Cl$ )/ $C_2H_2$  systems. These ion counts are clearly absent in the control experiments. Therefore, we can conclude that products detected via  $m/z = 165$  and  $166$  are formed, respectively, in the reactive [R9] and [R10] systems. Accounting for the molecular weight of the reactants and products (Scheme 2), the formation of the  $C_{13}H_{10}$  ( $m/z = 166$ ) isomer(s) is the result of the bimolecular reaction of 1'-/2'-methylnaphthyl ( $C_{11}H_9^\bullet$ ,  $m/z = 141$ ) with acetylene ( $C_2H_2$ ,  $m/z = 26$ ) followed by atomic hydrogen loss. The signal for  $C_{13}H_9^\bullet$  ( $m/z = 165$ ) can be attributed to hydrogen atom loss of  $C_{13}H_{10}$  ( $m/z = 166$ ) either by unimolecular decomposition or through hydrogen abstraction in the high temperature reactor. Note that ion counts at  $m/z = 139$  ( $C_{11}H_7^+$ ),  $140$  ( $C_{11}H_8^+$ ),  $142$  ( $^{13}CC_{10}H_9^+/C_{11}H_{10}^+$ ),  $143$  ( $^{13}CC_{10}H_{10}^+$ ),  $176$  ( $C_{11}H_9^{35}Cl^+$ ),  $177$  ( $^{13}CC_{10}H_9^{35}Cl^+$ ),  $178$  ( $C_{11}H_9^{37}Cl^+$ ), and  $179$  ( $^{13}CC_{10}H_9^{37}Cl^+$ ) are also detectable in the control experiments (Figs. 1a, c). These can be connected to the reactants ( $m/z = 176 - 179$ ), 1- and/or 2-methylnaphthalene ( $m/z = 142$ ,  $C_{11}H_{10}$ ), and stepwise hydrogen atom loss products of 1'-/2'-methylnaphthyl ( $m/z = 140$  and  $139$ ). Finally, we have a closer look at [R11] (Figs. 1e/f). Atomic chlorine formed via thermolysis of oxalyl chloride ( $C_2Cl_2O_2$ ) abstracts atomic hydrogen from the methyl group of 2'-methylbiphenyl ( $C_{13}H_{12}$ ) forming the 2'-methylbiphenyl radical ( $C_{13}H_{11}^\bullet$ ). This radical can be regarded as an ortho-phenyl substituted benzyl radical. As revealed in the test reaction of chlorine atoms with toluene ( $C_6H_5CH_3$ ) (Supplementary Information, Section 2) followed by reaction with acetylene ( $C_2H_2$ ) and formation of indene ( $C_9H_8$ ), hydrogen abstraction is essentially dominated from the methyl group resulting in a benzyl radical ( $C_6H_5CH_2^\bullet$ ), but not from the aromatic C-H moieties to the methyltolyl radical ( $C_6H_4^\bullet CH_3$ ). The preferred hydrogen abstraction from the methyl group is supported by the weaker C-H methyl compared to the aromatic C-H bonds,  $555 \text{ kJ}\cdot\text{mol}^{-1}$  versus  $656\text{-}700 \text{ kJ}\cdot\text{mol}^{-1}$ .<sup>47</sup> A comparison of [R11] (Fig. 1f) with the blank experiments reveals prominent ion counts at  $m/z = 166$  ( $C_{13}H_{10}^+$ ) and  $165$  ( $C_{13}H_9^+$ ), which are not present in the blank experiment. Ion counts at  $m/z = 168$  – the 2'-methylbiphenyl ( $C_{13}H_{12}$ ) is reduced in Fig. 1f compared to Fig. 1e due to hydrogen abstraction, while ion counts at  $m/z = 167$  ( $^{13}CC_{12}H_{10}^+/C_{13}H_{11}^+$ ) emerge. The molecular mass of the reactant (2'-methylbiphenyl radical,

$C_{13}H_{11}^{\bullet}$ , 167 amu) suggests that the product observed at  $m/z = 166$  ( $C_{13}H_{10}^+$ ) has one hydrogen atom less than the reactant, while ion counts at  $m/z = 165$  ( $C_{13}H_9^+$ ) could yet be the result of another hydrogen abstraction from the  $C_{13}H_{10}$  hydrocarbon.

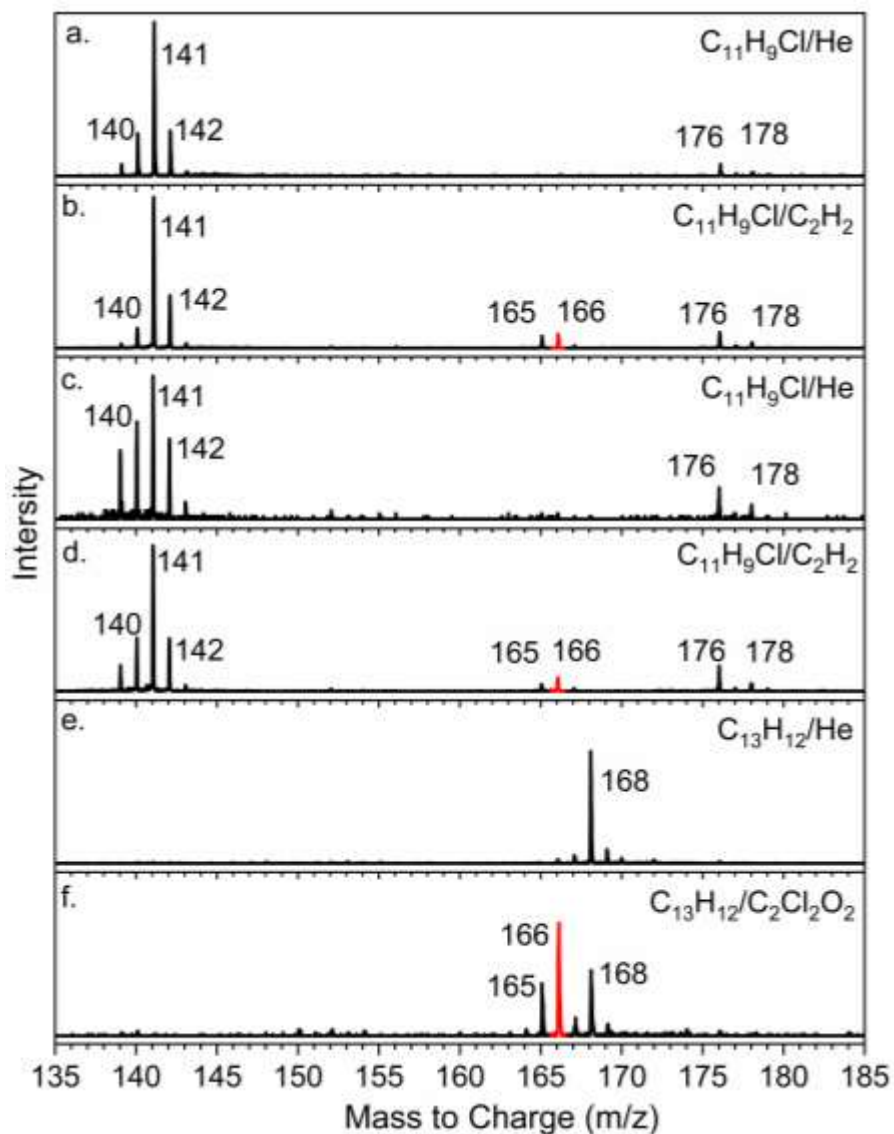


**Figure 1.** Mass spectra recorded at the photon energies of 10.00 eV for experiments (a-d) and 9.00 eV for experiments (e-f). (a) 1'-chloromethylnaphthalene ( $C_{11}H_9Cl$ )/helium (He) system at 1,023 K; (b) 1'-chloromethylnaphthalene ( $C_{11}H_9Cl$ )/acetylene ( $C_2H_2$ ) system at 1,023 K [R9]; (c) 2'-chloromethylnaphthalene ( $C_{11}H_9Cl$ )/helium (He) system at 973 K; (d) 2'-chloromethylnaphthalene ( $C_{11}H_9Cl$ )/acetylene ( $C_2H_2$ ) system at 973 K [R10]; (e) 2-methylbiphenyl

(C<sub>13</sub>H<sub>12</sub>)/helium (He) system at 1,023 K; (f) 2-methylbiphenyl (C<sub>13</sub>H<sub>12</sub>)/oxalyl chloride (C<sub>2</sub>Cl<sub>2</sub>O<sub>2</sub>) system at 1,023 K [11]. The ion signal highlighted in red relate to the products of interest (Scheme 2).

### 3.2. Photoionization Efficiency (PIE) Curves

It is our goal now not to only assign the molecular formulae of the reaction products (3.1.), but also to elucidate the product isomer(s). PIE curves, which report the ion counts at a well-defined  $m/z$  ratio versus the photon energy represent an ideal tool to accomplish this goal. These PIE curves can be fit with a linear combination of base functions, where each base function represents the PIE curve of a known isomers.<sup>23</sup> In this sense, the results from this linear combination provide explicit information of the isomers formed in this process. Therefore, the PIE calibration curves at  $m/z = 166$ <sup>23</sup> can be adopted to distinguish the C<sub>13</sub>H<sub>10</sub> isomers formed in reactions [R9] to [R11] (Fig. 2). The experimental PIE curves along with the fits are shown for  $m/z = 165, 166$  and  $167$  from 6.40 to 10.00 eV. Let us inspect the outcome of [R9] first (Figs. 2a-c). The PIE curve at  $m/z = 166$  had to be fit with three components: a dominating ( $86.7 \pm 8.7$  %) contribution from 3H-cyclopenta[a]naphthalene with minor fractions of 1H-cyclopenta[a]naphthalene (C<sub>13</sub>H<sub>10</sub>,  $5.3 \pm 0.5$  %) and the <sup>13</sup>CC<sub>12</sub>H<sub>9</sub>• radical ( $8.1 \pm 0.8$  %) at 9.00 eV with the percentage values referring to the total ion counts at  $m/z = 166$ . The PIE calibration curves of the C<sub>13</sub>H<sub>10</sub> isomers were taken from Reference<sup>23</sup>; considering 1.08 % of the natural abundance of the <sup>13</sup>C isotope, 14.16 % of ion counts for  $m/z = 165$  (C<sub>13</sub>H<sub>9</sub>•) contribute to the signal at  $m/z = 166$ . Due to the low fraction of ion counts connected to the <sup>13</sup>CC<sub>12</sub>H<sub>9</sub>• radical, the ion counts at  $m/z = 166$  from 6.50 to 7.50 eV are very low. The intensity rise at  $7.50 \pm 0.05$  eV can be connected to the adiabatic ionization energy (IE) of 1H-cyclopenta[a]naphthalene (IE= $7.45 \pm 0.05$  eV<sup>23</sup>). Contributions from 3H-cyclopenta[a]naphthalene (IE =  $7.60 \pm 0.05$  eV<sup>23</sup>) are required to match the total fit of the experimental PIE curve beyond  $7.60 \pm 0.05$  eV. Overall, in [R9], both 3H-cyclopenta[a]naphthalene and 1H-cyclopenta[a]naphthalene are synthesized under our experimental conditions. Note that ion counts at  $m/z = 167$  (<sup>13</sup>CC<sub>12</sub>H<sub>10</sub>) can be fit with the same overall

branching ratios of the ion counts for 3H-cyclopenta[a]naphthalene and 1H-cyclopenta[a]naphthalene, too. *Second*, the outcome of reaction [R10] is investigated (Figs. 2d-f). Here, the experimentally recorded PIE curve at  $m/z = 166$  could be also fit with three base functions: a dominating contribution of 3H-cyclopenta[a]naphthalene ( $C_{13}H_{10}$ ,  $85.3 \pm 8.5$  %) <sup>23</sup> and minor fractions of 1H-cyclopenta[b]naphthalene ( $C_{13}H_{10}$ ,  $7.6 \pm 0.8$  %) <sup>23</sup> along with the  $^{13}C_{12}H_9^{\bullet}$  radical at 9.00 eV. Accounting for the natural isotopic abundance of  $^{13}C$ , a fraction 14.16 % of the ion counts for  $m/z = 165$  ( $C_{13}H_9^{\bullet}$ ) (Fig. 2d) was added to the fit of the PIE curve at  $m/z = 166$ . *Finally*, the PIE curves collected for  $m/z = 165$  to 167 for [R11] (Figs. 2g-i) are quite distinct from those obtained for [R9] (Figs. 2a-c) and [R10] (Figs. 2d-f). For  $m/z = 166$ , a two-channel fit can replicate the experimental data: a dominating contribution from fluorene ( $C_{13}H_{10}$ ,  $94.5 \pm 9.5$  % at 9.00 eV) and a minor contribution from the  $^{13}C$ -substituted  $C_{13}H_9^{\bullet}$  radical recorded at  $m/z = 165$ . Note that the PIE curve at  $m/z = 167$  cannot be solely replicated through  $^{13}C$  contributions from  $^{13}C$ -fluorene ( $^{13}C_{12}H_{10}$ ); the remaining ion counts could originate from ionized 2'-methylbiphenyl radicals ( $C_{13}H_{11}^{\bullet}$ ); however, a reference PIE curve of the 2'-methylbiphenyl radical is not available. *Overall*, a detailed analysis of the PIE curves reveals the formation of four distinct  $C_{13}H_{10}$  isomer: 3H-cyclopenta[a]naphthalene, 1H-cyclopenta[a]naphthalene, 1H-cyclopenta[b]naphthalene, and fluorene. The PIE curves for  $m/z = 140, 141, 142, 143, 168, 169, 176$  and 178 are compiled in Figs. S5-S7 and discussed in the Supplementary Material along with the PIE curves at  $m/z = 165$  (Figs. 2a, d, and g; Supplementary Material, Fig. S8).

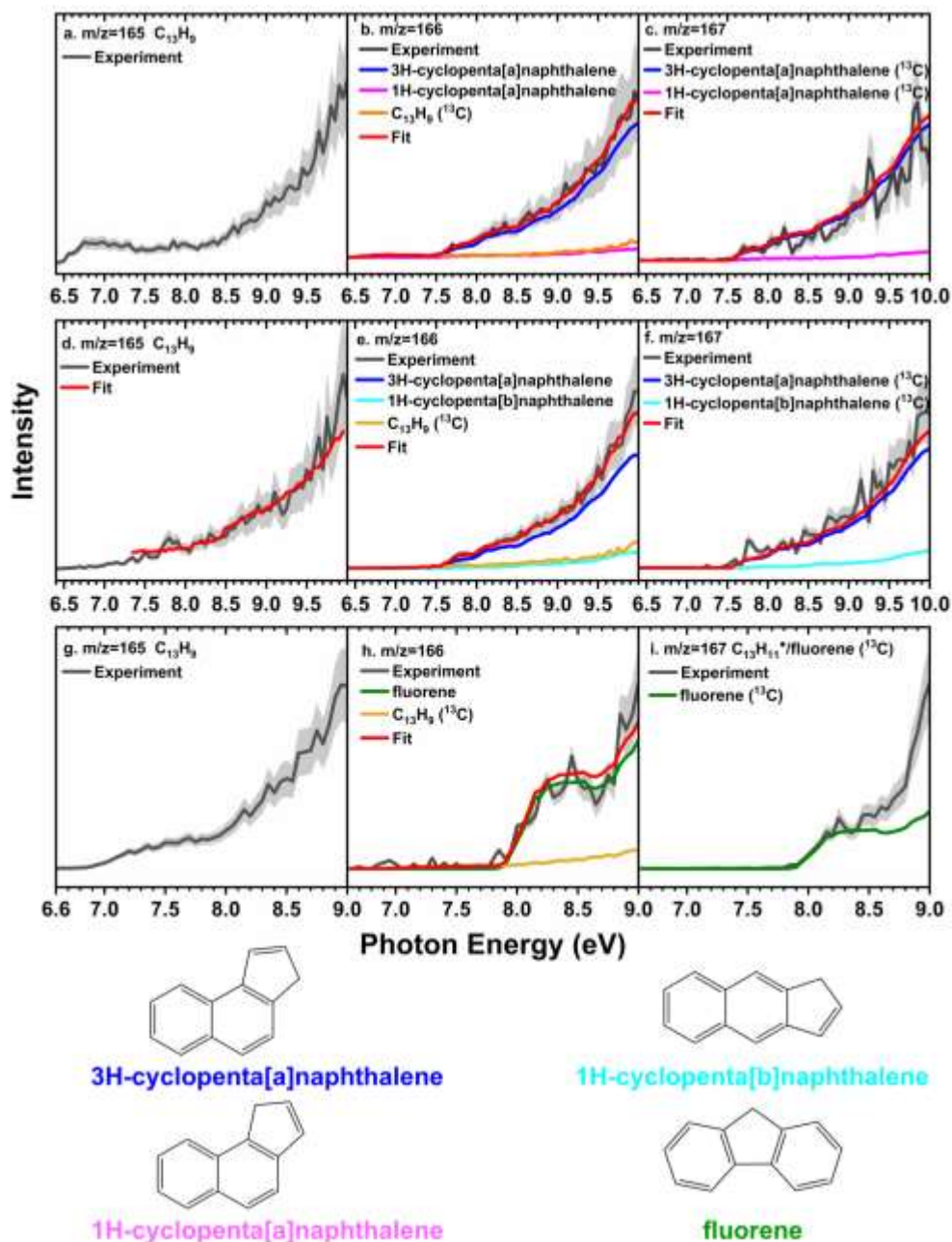


**Figure 2.** Experimental and reference PIE curves for species at  $m/z = 165$ ,  $166$  and  $167$ . (a-c) 1'-chloromethylnaphthalene ( $C_{11}H_9Cl-1$ )/acetylene ( $C_2H_2$ ) system at 1,023 K [R9]; (d-f) 2'-chloromethylnaphthalene ( $C_{11}H_9Cl-2$ )/acetylene ( $C_2H_2$ ) system at 973 K [R10]; (g-i) 2-methylbiphenyl ( $C_{13}H_{12}$ )/oxalyl chloride ( $C_2Cl_2O_2$ ) system at 1,023 K [R11]. The black line refers to the normalized experimental data with  $1 \sigma$  error limits defined in the shaded area. The colored lines refer to the reference PIE curves of isomers. The red line shows the overall fit via the linear combination of the reference curves. The reference data (red line) in Fig. 2h are from Reference <sup>23</sup>.

### 3.2. Reaction Mechanism

With the isomer-specific identification four distinct  $C_{13}H_{10}$  isomers - 1H-cyclopenta[a]naphthalene (**p1**), 3H-cyclopenta[a]naphthalene (**p2**), 1H-cyclopenta[b]naphthalene (**p3**), and fluorene (**p4**), we are turning our attention now to the underlying reaction pathways (Fig. 3). For reactions [R9] and [R10], a comparison of the molecular structures of the 1'-methylnaphthyl ( $C_{11}H_9^\bullet$ )/acetylene ( $C_2H_2$ ) and 2'-methylnaphthyl ( $C_{11}H_9^\bullet$ )/acetylene ( $C_2H_2$ ) reactants with the reaction products, i.e. 3H-cyclopenta[a]naphthalene (**p2**)/1H-cyclopenta[a]naphthalene (**p1**) and 3H-cyclopenta[a]naphthalene (**p2**)/1H-cyclopenta[b]naphthalene (**p3**), respectively, suggests an initial addition of the acetylene molecule with one carbon atom to the radical center at the  $-CH_2^\bullet$  moiety leading to two distinct  $C_{13}H_{11}^\bullet$  radical intermediates **i1** and **i2** carrying each a C3 side chain. These processes involve barriers to addition of 41 and 42  $\text{kJ}\cdot\text{mol}^{-1}$ , respectively.<sup>48</sup> This barrier is slightly below the barrier to addition of acetylene to the benzyl radical ( $C_6H_5CH_2^\bullet$ ) of 51  $\text{kJ}\cdot\text{mol}^{-1}$  as explored previously.<sup>1</sup> Intermediates **i1** and **i2** undergo cyclization to **i3** and **i4/i5**, respectively, passing barriers between 45 and 52  $\text{kJ}\cdot\text{mol}^{-1}$ . These intermediates can undergo atomic hydrogen loss to form three distinct cyclopentanaphthalenes: 1H-cyclopenta[a]naphthalene (**p1**), 3H-cyclopenta[a]naphthalene (**p2**), 1H-cyclopenta[b]naphthalene (**p3**); note that **i3** may also isomerize via hydrogen atom shift to **i6** prior to carbon-hydrogen bond rupture forming 3H-cyclopenta[a]naphthalene (**p2**). Finally, considering reaction [R11], a ring closure through a substantial barrier of 101  $\text{kJ}\cdot\text{mol}^{-1}$  leads to intermediate **i7**, which then can eject atomic hydrogen to the fluorene (**p4**) isomer. Although the overall reactions forming **p1** - **p4** are exoergic, the entrance barriers to addition ([R9]/[R10]) and ring closure ([R11]) block these reactions at low temperatures such as in molecular clouds (10 K) and in hydrocarbon rich atmospheres of planets and their moons like Titan (94 – 200 K); elevated temperatures such as in combustion flames and in carbon-rich circumstellar envelopes, e.g. of IRC+10,216 are required to efficiently overcome the barriers to addition.

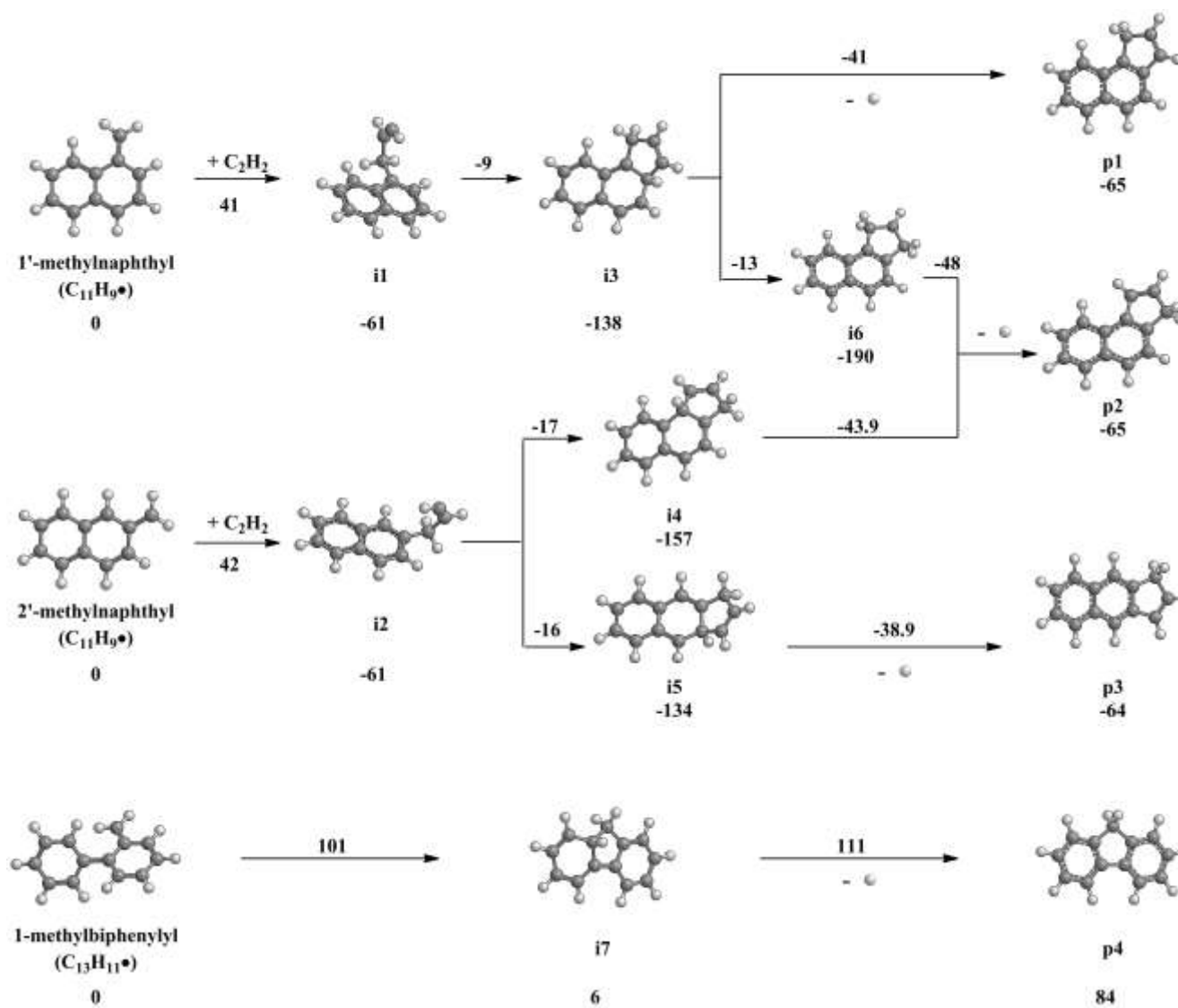


**Figure 3.** Computed reaction pathways to four distinct  $C_{13}H_{10}$  isomers 1H-cyclopenta[a] naphthalene (**p1**), 3H-cyclopenta[a]naphthalene (**p2**), 1H-cyclopenta[b]naphthalene (**p3**), and fluorene (**p4**) compiled from Reference <sup>48</sup>.



## 4. Conclusions

The explicit detection of four distinct  $C_{13}H_{10}$  isomers 1H-cyclopenta[a]naphthalene (**p1**), 3H-cyclopenta[a]naphthalene (**p2**), 1H-cyclopenta[b]naphthalene (**p3**), and fluorene (**p4**) along with their underlying reaction mechanisms has far reaching implications to the formation of PAHs carrying five-membered rings at elevated temperatures such as in combustion flames and in carbon-rich circumstellar envelopes along with planetary nebulae as their descendants. *First*, our studies propose that *any* PAH with a methylated six-membered ring can undergo molecular mass growth processes and annulation by a five-membered ring after hydrogen abstraction from the methyl group and successive reaction with acetylene as long as a hydrogen atom is attached to one of the neighboring carbon atoms in the ortho position (Fig. 4). Note that in deep space, energetic UV photons can also initiate the C-H bond cleavage at the methyl group.<sup>49, 50</sup> The origin of the organic side chain (methyl group) to aromatics represents a different line of research. Previous studies suggest that the addition of a methyl group to benzene followed by hydrogen atom loss is endoergic by  $37.2 \text{ kJ}\cdot\text{mol}^{-1}$  and has to pass an entrance barrier of  $53.5 \text{ kJ}\cdot\text{mol}^{-1}$ .<sup>51</sup> This results to low reaction rates of only  $5.42\times 10^{-22}$ - $1.38\times 10^{-14} \text{ cm}^3\cdot\text{molecules}^{-1}\cdot\text{s}^{-1}$  in the temperature range from 300 K to 1,100 K. Alternatively, crossed molecular beam experiments of ethynyl ( $C_2H^\bullet$ ) radicals with 1-methyl- and 2-methyl-1,3-butadiene ( $C_5H_8$ ) are rapid, overall exoergic, and reveal pathways to toluene ( $C_6H_5CH_3$ ) without entrance barrier.<sup>52-54</sup> Likewise, as demonstrated in crossed molecular beam experiments, the 1-propynyl radical ( $CH_3CC$ ) reacting with 1,3-butadiene ( $C_4H_6$ ) leads to toluene ( $C_6H_5CH_3$ ) without entrance barrier.<sup>55</sup> Note that the benzyl radical ( $C_6H_5CH_2^\bullet$ ) can be accessed barrierlessly via the bimolecular reaction of dicarbon ( $C_2$ ) with 2-methyl-1,3-butadiene ( $C_5H_8$ ) thus bypassing the classical hydrogen abstraction pathway.<sup>56</sup> *Second*, the methylene ( $CH_2$ ) moiety at the newly formed five-membered ring can undergo facile C-H bond cleavage either upon photolysis or hydrogen abstraction forming a resonantly stabilized cyclopentadienyl radical moiety (Fig. 4). Recent molecular beam experiments revealed that cyclopentadienyl ( $C_5H_5^\bullet$ )<sup>57</sup> and 1-indenyl ( $C_9H_7^\bullet$ ),<sup>58</sup> which also carries a cyclopentadienyl unit,

undergo ring expansion from a five- to a six membered ring upon reaction with methyl ( $\text{CH}_3^\bullet$ ) radicals. Altogether, this chain of reactions eventually converts a methyl group via a five-membered ring PAH to a six-membered benzene ring thus effectively transiting molecular building blocks relevant to the formation of three-dimensional carbonaceous nanostructures to those of critical importance to graphene-type two-dimensional nano-sheets at elevated temperatures.

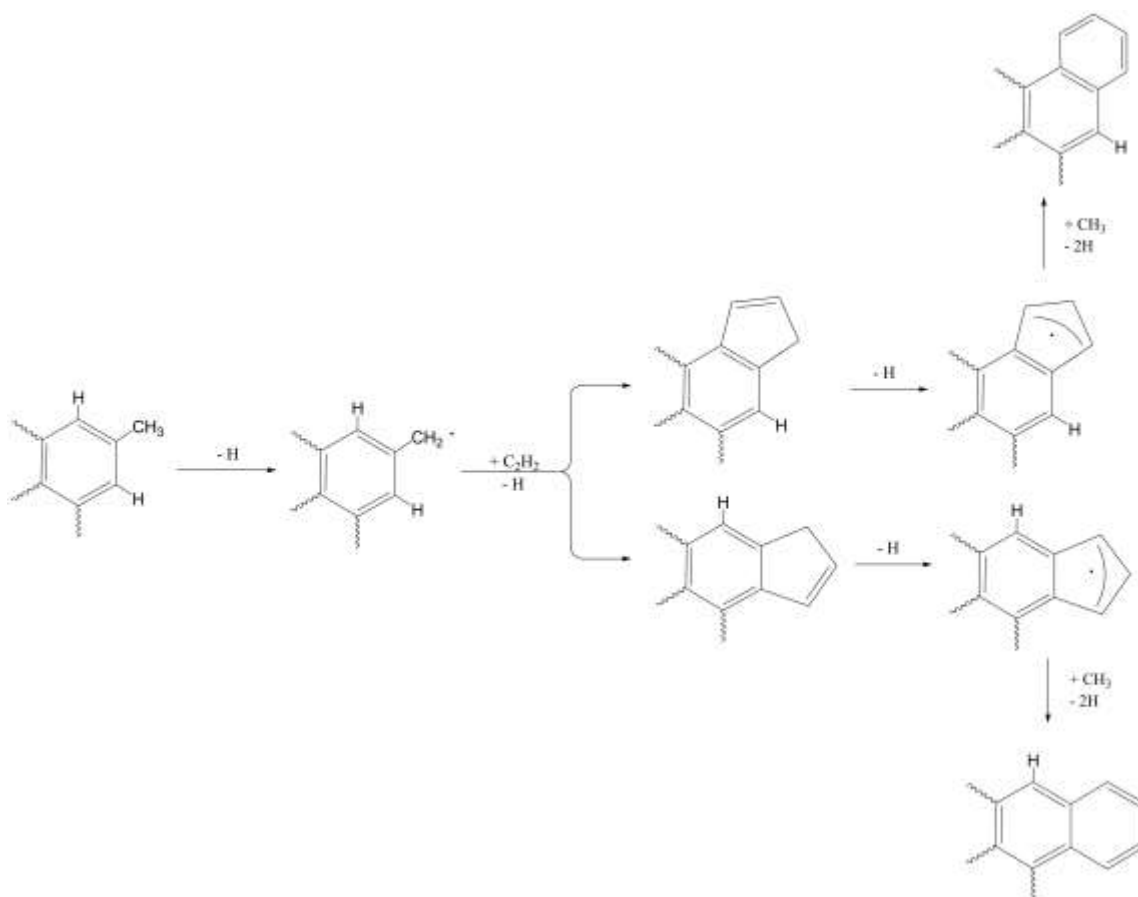


**Figure 4.** Molecular mass growth processes involving a methyl side group via five-membered rings to benzannulation of a PAH.

### Acknowledgements

The authors are grateful for the funding supports from National Natural Science Foundation of China (22173091). This work is based on proposal 2022-HLS-PT-004982 (RIK); RIK acknowledges support from the U.S. Department of Energy, Basic Energy Sciences DE-FG02-

03ER15411.

## Reference.

- (1) Parker, D. S.; Kaiser, R. I.; Kostko, O.; Ahmed, M., Selective formation of indene through the reaction of benzyl radicals with acetylene. *Chemphyschem* **2015**, *16* (10), 2091-2093.
- (2) Josa, D.; Azevedo dos Santos, L.; González-Veloso, I.; Rodríguez-Otero, J.; Cabaleiro-Lago, E. M.; de Castro Ramalho, T., Ring-annelated corannulenes as fullerene receptors. A DFT-D study. *RSC Adv.* **2014**, *4* (56), 29826-29833.
- (3) Becker, L.; Bunch, T. E., Fullerenes, fullerenes and polycyclic aromatic hydrocarbons in the allende meteorite. *Meteorit Planet Sci.* **1997**, *32* (4), 479-487.
- (4) Devi, G.; Buragohain, M.; Pathak, A., DFT study of five-membered ring PAHs. *Planet. Space Sci.* **2020**, *183*, 104593.
- (5) Doddipatlal, S.; Galimova, G. R.; Wei, H.; Thomas, A. M.; He, C.; Yang, Z.; Morozov, A. N.; Shingledecker, C. N.; Mebel, A. M.; Kaiser, R. I., Low-temperature gas-phase formation of indene in the interstellar medium. *Sci. Adv.* **2021**, *7* (1), eabd4044.
- (6) Richter, H.; Grieco, W. J.; Howard, J. B., Formation mechanism of polycyclic aromatic hydrocarbons and fullerenes in premixed benzene flames. *Combust. Flame* **1999**, *119* (1-2), 1-22.
- (7) Hansen, N.; Klippenstein, S. J.; Miller, F. J.; Wang, J.; Cool, T. A.; Law, M. E.; Westmoreland, P. R.; Kasper, T.; Kohse-Höinghaus, K., Identification of C<sub>5</sub>H<sub>x</sub> isomers in fuel-rich flames by photoionization mass spectrometry and electronic structure calculations. *J. Phys. Chem. A* **2006**, *106* (13), 4376-4388.
- (8) Ruwe, L.; Cai, L.; Moshhammer, K.; Hansen, N.; Pitsch, H.; Kohse-Höinghaus, K., The C<sub>5</sub> chemistry preceding the formation of polycyclic aromatic hydrocarbons in a premixed 1-pentene flame. *Combust. Flame* **2019**, *206*, 411-423.
- (9) Yang, B.; Li, Y.; Wei, L.; Huang, C.; Wang, J.; Tian, Z.; Yang, R.; Sheng, L.; Zhang, Y.; Qi, F., An experimental study of the premixed benzene/oxygen/argon flame with tunable synchrotron photoionization. *Proc. Combust. Inst.* **2007**, *31* (1), 555-563.
- (10) Hansen, N.; Cool, T. A.; Westmoreland, P. R.; Kohse-Höinghaus, K., Recent contributions of flame-sampling molecular-beam mass spectrometry to a fundamental understanding of combustion chemistry. *Prog. Energy Combust. Sci.* **2009**, *35* (2), 168-191.
- (11) Xu, L.; Yan, F.; Wang, Y., A comparative study of the sooting tendencies of various C<sub>5</sub>-C<sub>8</sub> alkanes, alkenes and cycloalkanes in counterflow diffusion flames. *Appl. Energy Combust. Sci.* **2020**, *1-4*, 100007.
- (12) Kohse-Höinghaus, K.; Atakan, B.; Lamprecht, A.; González Alatorre, G.; Kamphus, M.; Kasper, T.; Liu, N., Contributions to the investigation of reaction pathways in fuel-rich flames. *Phys. Chem. Chem. Phys.* **2002**, *4* (11), 2056-2062.
- (13) Lamprecht, A.; Atakan, B.; Kohse-Höinghaus, K., Fuel-rich flame chemistry in low-pressure cyclopentene flames. *Proc. Combust. Inst.* **2000**, *28* (2), 1817-1824.
- (14) Hansen, N.; Kasper, T.; Klippenstein, S. J.; Westmoreland, P. R.; Law, C. K.; Taatjes, C. A.; Kohse-Höinghaus, K.; Wang, J.; Cool, T. A., Initial steps of aromatic ring formation in a laminar premixed fuel-rich cyclopentene flame. *J. Phys. Chem. A* **2007**, *111* (19), 4081-4092.

- (15) Taatjes, C. A.; Klippenstein, S. J.; Hansen, N.; Miller, J. A.; Cool, T. A.; Wang, J.; Law, M. E.; Westmoreland, P. R., Synchrotron photoionization measurements of combustion intermediates: photoionization efficiency and identification of C<sub>3</sub>H<sub>2</sub> isomers. *Phys. Chem. Chem. Phys.* **2005**, *7* (5), 806-13.
- (16) Hansen, N.; Klippenstein, S. J.; Westmoreland, P. R.; Kasper, T.; Kohse-Hoinghaus, K.; Wang, J.; Cool, T. A., A combined ab initio and photoionization mass spectrometric study of polyynes in fuel-rich flames. *Phys. Chem. Chem. Phys.* **2008**, *10* (3), 366-74.
- (17) Jin, H.; Xing, L.; Hao, J.; Yang, J.; Zhang, Y.; Cao, C.; Pan, Y.; Farooq, A., A chemical kinetic modeling study of indene pyrolysis. *Combust. Flame* **2019**, *206*, 1-20.
- (18) Shao, C.; Kukkadapu, G.; Wagnon, S. W.; Pitz, W. J.; Sarathy, S. M., PAH formation from jet stirred reactor pyrolysis of gasoline surrogates. *Combust. Flame* **2020**, *219*, 312-326.
- (19) Liu, P.; Li, Z.; Roberts, W. L., Growth network of PAH with 5-membered ring: Case study with acenaphthylene molecule. *Combust. Flame* **2021**, *230*, 111449.
- (20) Wang, H.; Liu, Z.; Gong, S.; Liu, Y.; Wang, L.; Zhang, X.; Liu, G., Experimental and kinetic modeling study on 1,3-cyclopentadiene oxidation and pyrolysis. *Combust. Flame* **2020**, *212*, 189-204.
- (21) Hansen, N.; Schenk, M.; Moshhammer, K.; Kohse-Höinghaus, K., Investigating repetitive reaction pathways for the formation of polycyclic aromatic hydrocarbons in combustion processes. *Combust. Flame* **2017**, *180*, 250-261.
- (22) Schenk, M.; Hansen, N.; Vieker, H.; Beyer, A.; Gölzhäuser, A.; Kohse-Höinghaus, K., PAH formation and soot morphology in flames of C<sub>4</sub> fuels. *Proc. Combust. Inst.* **2015**, *35* (2), 1761-1769.
- (23) Zhao, L.; Prendergast, M.; Kaiser, R. I.; Xu, B.; Ablikim, U.; Lu, W.; Ahmed, M.; Oleinikov, A. D.; Azyazov, V. N.; Howlander, A. H.; Wnuk, S. F.; Mebel, A. M., How to add a five-membered ring to polycyclic aromatic hydrocarbons (PAHs) - molecular mass growth of the 2-naphthyl radical (C<sub>10</sub>H<sub>7</sub>) to benzindenes (C<sub>13</sub>H<sub>10</sub>) as a case study. *Phys. Chem. Chem. Phys.* **2019**, *21* (30), 16737-16750.
- (24) Cherchneff, I., The formation of polycyclic aromatic hydrocarbons in evolved circumstellar environments. *EAS Publications Series* **2011**, *46*, 177-189.
- (25) Parker, D. S.; Zhang, F.; Kim, Y. S.; Kaiser, R. I.; Landera, A.; Kislov, V. V.; Mebel, A. M.; Tielens, A. G., Low temperature formation of naphthalene and its role in the synthesis of PAHs (polycyclic aromatic hydrocarbons) in the interstellar medium. *Proc. Natl. Acad. Sci. U.S.A.* **2012**, *109* (1), 53-58.
- (26) McCabe, M. N.; Hemberger, P.; Reusch, E.; Bodi, A.; Bouwman, J., Off the beaten path: Almost clean formation of indene from the ortho-benzyne + allyl reaction. *J. Phys. Chem. Lett.* **2020**, *11* (8), 2859-2863.
- (27) Zhang, F.; Kaiser, R. I.; Kislov, V. V.; Mebel, A. M.; Golan, A.; Ahmed, M., A VUV photoionization study of the formation of the indene molecule and its isomers. *J. Phys. Chem. Lett.* **2011**, *2* (14), 1731-1735.
- (28) Parker, D. S.; Zhang, F.; Kaiser, R. I.; Kislov, V. V.; Mebel, A. M., Indene formation under single-collision conditions from the reaction of phenyl radicals with allene and methylacetylene-A crossed molecular beam and ab initio study. *Chem. Asian J.* **2011**, *6* (11), 3035-3047.
- (29) Kukkadapu, G.; Wagnon, S. W.; Pitz, W. J.; Hansen, N., Identification of the molecular-weight growth reaction network in counterflow flames of the C<sub>3</sub>H<sub>4</sub> isomers allene and propyne. *Proc. Combust. Inst.* **2021**, *38* (1), 1477-1485.
- (30) Kaiser, R. I.; Hansen, N., An aromatic universe-A physical chemistry perspective. *J. Phys. Chem. A* **2021**, *125* (18), 3826-3840.

- (31) Zhao, L.; Kaiser, R. I.; Xu, B.; Ablikim, U.; Ahmed, M.; Evseev, M. M.; Bashkirov, E. K.; Azyazov, V. N.; Mebel, A. M., Low-temperature formation of polycyclic aromatic hydrocarbons in Titan's atmosphere. *Nat. Astron.* **2018**, *2* (12), 973-979.
- (32) Zhang, F.; Kim, Y. S.; Kaiser, R. I.; Krishtal, S. P.; Mebel, A. M., Crossed molecular beams study on the formation of vinylacetylene in Titan's atmosphere. *J. Phys. Chem. A* **2009**, *113* (42), 11167-11173.
- (33) Zhao, L.; Kaiser, R. I.; Lu, W.; Ahmed, M.; Oleinikov, A. D.; Azyazov, V. N.; Mebel, A. M.; Howlader, A. H.; Wnuk, S. F., Gas phase formation of phenalene via  $10\pi$ -aromatic, resonantly stabilized free radical intermediates. *Phys. Chem. Chem. Phys.* **2020**, *22* (27), 15381-15388.
- (34) Moriarty, N. W.; Frenklach, M., AB into study of naphthalene formation by addition of vinylacetylene to phenyl. *Proc. Combust. Inst.* **2000**, *28* (2), 2563-2568.
- (35) Zhao, L.; Prendergast, M. B.; Kaiser, R. I.; Xu, B.; Lu, W.; Ablikim, U.; Ahmed, M.; Oleinikov, A. D.; Azyazov, V. N.; Mebel, A. M.; Howlader, A. H.; Wnuk, S. F., Reactivity of the indenyl radical ( $C_9H_7$ ) with acetylene ( $C_2H_2$ ) and vinylacetylene ( $C_4H_4$ ). *Chemphyschem* **2019**, *20* (11), 1437-1447.
- (36) Zhao, L.; Kaiser, R. I.; Xu, B.; Ablikim, U.; Ahmed, M.; Evseev, M. M.; Bashkirov, E. K.; Azyazov, V. N.; Mebel, A. M., A unified mechanism on the formation of acenes, helicenes, and phenacenes in the gas phase. *Angew. Chem. Int. Ed.* **2020**, *59* (10), 4051-4058.
- (37) Zhao, L.; Kaiser, R. I.; Xu, B.; Ablikim, U.; Ahmed, M.; Zagidullin, M. V.; Azyazov, V. N.; Howlader, A. H.; Wnuk, S. F.; Mebel, A. M., VUV photoionization study of the formation of the simplest polycyclic aromatic hydrocarbon: naphthalene ( $C_{10}H_8$ ). *J. Phys. Chem. Lett.* **2018**, *9* (10), 2620-2626.
- (38) Couch, D. E.; Zhang, A. J.; Taatjes, C. A.; Hansen, N., Experimental observation of hydrocarbon growth by resonance-stabilized radical-radical chain reaction. *Angew. Chem. Int. Ed.* **2021**, *60* (52), 27230-27235.
- (39) Zhao, L.; Kaiser, R. I.; Lu, W.; Kostko, O.; Ahmed, M.; Evseev, M. M.; Bashkirov, E. K.; Oleinikov, A. D.; Azyazov, V. N.; Mebel, A. M.; Howlader, A. H.; Wnuk, S. F., Gas phase formation of cyclopentanaphthalene (benzindene) isomers via reactions of 5- and 6-indenyl radicals with vinylacetylene. *Phys. Chem. Chem. Phys.* **2020**, *22* (39), 22493-22500.
- (40) Richter, H.; Mazyar, O. A.; Sumathi, R.; Green, W. H.; Howard, J. B.; Bozzelli, J. W., Detailed kinetic study of the growth of small polycyclic aromatic hydrocarbons. 1. 1-Naphthyl + Ethyne. *J. Phys. Chem. A* **2001**, *105* (9), 1561-1573.
- (41) Olten, N.; Senkan, S., Formation of polycyclic aromatic hydrocarbons in an atmospheric pressure ethylene diffusion flame. *Combust. Flame* **1999**, *118* (3), 500-507.
- (42) Li, Y.; Zhang, L.; Yuan, T.; Zhang, K.; Yang, J.; Yang, B.; Qi, F.; Law, C. K., Investigation on fuel-rich premixed flames of monocyclic aromatic hydrocarbons: Part I. Intermediate identification and mass spectrometric analysis. *Combust. Flame* **2010**, *157* (1), 143-154.
- (43) Zhang, T.; Zhang, L.; Hong, X.; Zhang, K.; Qi, F.; Law, C. K.; Ye, T.; Zhao, P.; Chen, Y., An experimental and theoretical study of toluene pyrolysis with tunable synchrotron VUV photoionization and molecular-beam mass spectrometry. *Combust. Flame* **2009**, *156* (11), 2071-2083.
- (44) Yuan, W.; Li, Y.; Dagaut, P.; Yang, J.; Qi, F., Investigation on the pyrolysis and oxidation of toluene over a wide range conditions. I. Flow reactor pyrolysis and jet stirred reactor oxidation. *Combust. Flame* **2015**, *162* (1), 3-21.
- (45) Zhou, Z.; Du, X.; Yang, J.; Wang, Y.; Li, C.; Wei, S.; Du, L.; Li, Y.; Qi, F.; Wang, Q., The vacuum

- ultraviolet beamline/endstations at NSRL dedicated to combustion research. *J. Synchrotron Radiat.* **2016**, *23* (4), 1035-45.
- (46) Zhao, L.; Yang, T.; Kaiser, R. I.; Troy, T. P.; Xu, B.; Ahmed, M.; Alarcon, J.; Belisario-Lara, D.; Mebel, A. M.; Zhang, Y.; Cao, C.; Zou, J., A vacuum ultraviolet photoionization study on high-temperature decomposition of JP-10 (exo-tetrahydrodicyclopentadiene). *Phys. Chem. Chem. Phys.* **2017**, *19* (24), 15780-15807.
- (47) Shanshal, M.; Muala, M. M., Reaction paths and transition states of C-H bond rupture in aromatics; benzene and toluene molecules. *Jordan J. C.* **2011**, *6* (2), 165-173.
- (48) Galimova, G. R.; Medvedkov, I. A.; Mebel, A. M., The role of methylaryl radicals in the growth of polycyclic aromatic hydrocarbons: The formation of five-membered rings. *J. Phys. Chem. A* **2022**, *126* (7), 1233-1244.
- (49) Kaiser, R. I.; Stranges, D.; Lee, Y. T.; Suits, A. G., Neutral-neutral reactions in the interstellar medium. 1. Formation of carbon hydride radicals via reaction of carbon atoms with unsaturated hydrocarbons. *Astrophys. J.* **1997**, *477* (2), 982-989.
- (50) Kaiser, R. I.; Lee, Y. T.; Suits, A. G., Crossed-beam reaction of  $C(^3P_1)$  with  $C_2H_2(^1\Sigma^+g)$ : Observation of tricarbon-hydride  $C_3H$ . *J. Chem. Phys.* **1995**, *103* (23), 10395-10398.
- (51) Kislov, V. V.; Mebel, A. M., Ab initio G3-type/statistical theory study of the formation of indene in combustion flames. I. Pathways involving benzene and phenyl radicals. *J. Phys. Chem. A* **2007**, *111* (19), 3922-3931.
- (52) Dangi, B. B.; Parker, D. S.; Kaiser, R. I.; Jamal, A.; Mebel, A. M., A combined experimental and theoretical study on the gas-phase synthesis of toluene under single collision conditions. *Angew. Chem. Int. Ed.* **2013**, *52* (28), 7186-7189.
- (53) Mebel, A. M.; Kaiser, R. I., Formation of resonantly stabilised free radicals via the reactions of atomic carbon, dicarbon, and tricarbon with unsaturated hydrocarbons: Theory and crossed molecular beams experiments. *Int. Rev. Phys. Chem.* **2015**, *34* (4), 461-514.
- (54) Kaiser, R. I.; Parker, D. S.; Mebel, A. M., Reaction dynamics in astrochemistry: Low-temperature pathways to polycyclic aromatic hydrocarbons in the interstellar medium. *Annu. Rev. Phys. Chem.* **2015**, *66* (1), 43-67.
- (55) Thomas, A. M.; He, C.; Zhao, L.; Galimova, G. R.; Mebel, A. M.; Kaiser, R. I., Combined experimental and computational study on the reaction dynamics of the 1-propynyl ( $CH_3CC$ )-1,3-butadiene ( $CH_2CHCHCH_2$ ) system and the formation of toluene under single collision conditions. *J. Phys. Chem. A* **2019**, *123* (19), 4104-4118.
- (56) Dangi, B. B.; Parker, D. S.; Yang, T.; Kaiser, R. I.; Mebel, A. M., Gas-phase synthesis of the benzyl radical ( $C_6H_5CH_2$ ). *Angew. Chem. Int. Ed.* **2014**, *53* (18), 4608-4613.
- (57) Kaiser, R. I.; Zhao, L.; Lu, W.; Ahmed, M.; Zagidullin, M. V.; Azyazov, V. N.; Mebel, A. M., Formation of benzene and naphthalene through cyclopentadienyl-mediated radical-radical reactions. *J. Phys. Chem. Lett.* **2022**, *13* (1), 208-213.
- (58) Zhao, L.; Kaiser, R. I.; Lu, W.; Xu, B.; Ahmed, M.; Morozov, A. N.; Mebel, A. M.; Howlader, A. H.; Wnuk, S. F., Molecular mass growth through ring expansion in polycyclic aromatic hydrocarbons via radical-radical reactions. *Nat. Commun.* **2019**, *10* (1), 3689.